

Magnetotransport properties of Fe₄₈Mn₂₄Ga₂₈ Heusler alloys

V. V. Khovaylo

National University of Science and Technology "MISIS," Moscow 119049, Russia

T. Omori, K. Endo, X. Xu, and R. Kainuma

Department of Materials Science, Graduate School of Engineering, Tohoku University, Sendai 980–8579, Japan

A. P. Kazakov, V. N. Prudnikov, E. A. Gan'shina, A. I. Novikov, Yu. O. Mikhailovsky, D. E. Mettus, and A. B. Granovsky

Faculty of Physics, M.V. Lomonosov Moscow State University, Moscow 119991, Russia

(Received 9 January 2013; revised manuscript received 26 March 2013; published 7 May 2013)

Magnetotransport properties of an Fe₄₈Mn₂₄Ga₂₈ Heusler-based ferromagnetic shape memory alloy are tracked in a temperature interval that covers both martensitic and austenitic phases. A large temperature hysteresis indicative of a coupled magnetostructural transition from ferromagnetic martensite to paramagnetic austenite is observed on the temperature dependencies of magnetization and electrical resistivity. The temperature dependency of the anomalous Hall-effect coefficient in Fe₄₈Mn₂₄Ga₂₈ cannot be described in terms of skew scattering, side-jump, and intrinsic mechanisms of the anomalous Hall-effect theory. The Hall-effect resistivity in the martensitic state is smaller, but is of the same order of magnitude as in the case of the giant Hall effect in a half-metallic Co₂MnAl. Specific features of the temperature dependencies of magnetization, resistivity, magnetoresistance, and ordinary and anomalous Hall-effect coefficients are discussed and the possible routes for increasing Hall-effect resistivity are suggested.

DOI: [10.1103/PhysRevB.87.174410](https://doi.org/10.1103/PhysRevB.87.174410)

PACS number(s): 75.47.Np, 72.15.Gd

I. INTRODUCTION

Mn-based ferromagnetic Heusler alloys are of considerable experimental and theoretical interest due primarily to a high spin polarization in the half-metallic alloys and giant magnetic-field-induced strains in the ferromagnetic shape memory alloys (see, for review, Refs. 1–5).

Recently, much effort has been devoted to the study of magnetotransport properties of Heusler alloys, particularly the anomalous Hall effect (AHE) in the Heusler-based half metals^{6–9} and ferromagnetic shape memory alloys.^{10–13} For both classes of materials, a giant Hall effect has been found,^{6,9,11} which can be used in magnetic sensors^{6,9} and also in the search for giant spin Hall effect because of their common origin. For the former class of materials, different mechanisms of AHE such as skew scattering⁷ and intrinsic contribution⁸ were considered to be the most important, despite the fact that these compounds belong to the high-resistivity alloys whose AHE, as a rule, exhibits behavior which cannot be explained in the framework of these mechanisms.¹⁴ For the latter class of materials, a number of intriguing features in the Hall effect have been reported to take place in a martensitic phase,¹⁰ as well as in the martensitic transformation interval where the low-temperature martensitic and high-temperature austenitic phases coexist.^{11,12} Specifically, a very large exponent n in a correlation between the saturated anomalous Hall resistivity ρ_A and the longitudinal resistivity ρ_{xx} , $\rho_A \sim \rho_{xx}^{n=4.2}$, has been suggested to originate from the presence of large Mn-rich clusters which enhance spin-dependent electron scattering in the martensitic phase of Ni-Mn(Fe)-Ga melt-spun ribbons.¹⁰ Peculiar magnetic field dependence and giant values of Hall resistivity observed in the two-phase coexistence region of a polycrystalline Ni-Mn-In alloy have been ascribed to a partial magnetic-field-induced

conversion of martensite into austenite and the existence of nanosized clusters of austenite whose concentration in the martensitic matrix is close to a percolation threshold, respectively.^{11,12} Recently, the ordinary and anomalous Hall-effect coefficients have been determined for Ni-Mn-In(Si) alloys and it has been shown that there are no abrupt changes in electronic structure at the martensitic transition.¹³ These findings indicate that ferromagnetic shape memory alloys are worth studying with respect to their magnetotransport properties.

One of the recently reported ferromagnetic materials undergoing martensitic transformation is Fe-Mn-Ga Heusler alloys.¹⁵ Magnetic and structural characterizations of a sample with an Fe₄₃Mn₂₈Ga₂₉ nominal composition showed that the martensitic transformation takes place from a paramagnetic L₂₁ cubic parent phase to a ferromagnetic L₁₀ tetragonal product phase.¹⁵ Magnetic measurements performed on an Fe₄₄Mn₂₈Ga₂₈ single crystalline sample revealed that the c axis of martensite is an easy magnetization axis.¹⁶ In the Fe-Mn-Ga alloys, a large thermal hysteresis of about 70 K between direct and reverse martensitic transformation is presumably conditioned by a comparatively large volume change at the martensitic transformation, $\Delta V \approx 0.7\text{--}1.35\%$ (Refs. 15 and 16).

The only reported result on the measurement of transport properties in Fe-Mn-Ga has shown that electrical resistivity ρ of the tetragonal martensitic phase is lower than that of the cubic austenitic phase.¹⁷ Moreover, in the high-temperature cubic phase, ρ demonstrates a slight tendency to decrease with increasing temperature. Such features are in apparent contradiction to transport properties of other Heusler-based ferromagnetic shape memory alloys. Therefore, there is a need for a deeper investigation of transport properties of the Fe-Mn-Ga alloy system.

II. SAMPLE PREPARATION AND MEASUREMENTS

Polycrystalline ingot of $\text{Fe}_{48}\text{Mn}_{24}\text{Ga}_{28}$ nominal composition was prepared by induction melting under a protective Ar atmosphere. Polycrystalline samples were obtained by hot rolling at 1273 K and subsequent annealing at 1273 K for 168 h. The x-ray diffraction pattern taken at room temperature showed that $\text{Fe}_{48}\text{Mn}_{24}\text{Ga}_{28}$ has a cubic structure. Due to the fact that Fe-Mn-Ga polycrystalline samples are very brittle, the specimen used for the measurements of magnetic and transport properties was a single crystalline grain taken from the polycrystalline sample. Magnetic measurements were carried out by a vibrating sample magnetometer (Lake Shore VSM 7400 System) in a temperature interval 80–400 K and by a magneto-optical setup in the geometry of the transverse Kerr effect. Longitudinal electrical resistivity, magneto-resistance, and Hall resistivity were measured by a standard four-probe technique in a temperature interval 80–320 K. Prior to the magnetic and magnetotransport measurements, the samples were subjected to at least three heating-cooling thermocycles in a temperature range 400–80 K. The magnetotransport measurements were carried out upon heating protocol after cooling the samples from 400 K to the starting temperature at zero magnetic field that corresponds to the zero-field-cooled (ZFC) measurements.

III. EXPERIMENTAL RESULTS AND DISCUSSION

Shown in Fig. 1 are the temperature dependencies of magnetization M measured upon heating and cooling in a magnetic field of 5 kOe. The drastic increase in magnetization

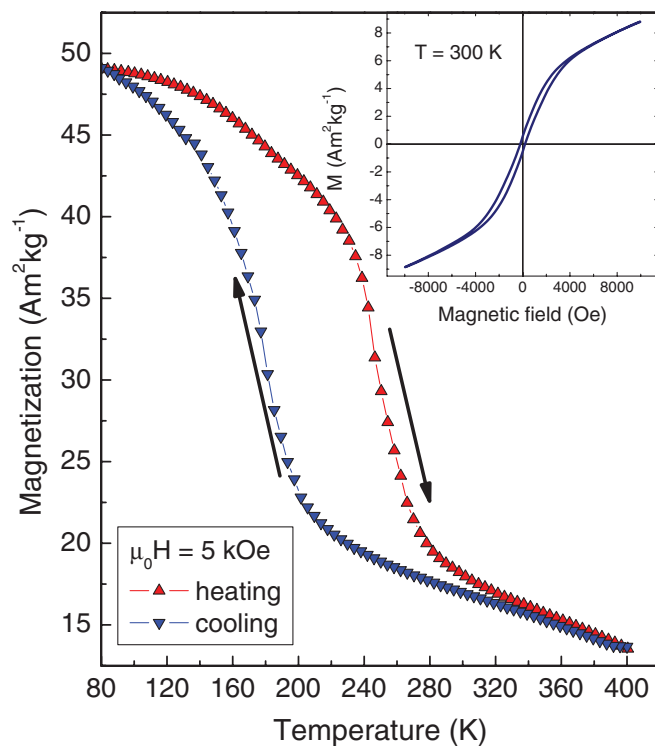


FIG. 1. (Color online) Temperature dependence of the magnetization M measured in a magnetic field $\mu_0 H = 5$ kOe. Shown in the inset is a magnetic hysteresis loop taken at 300 K.

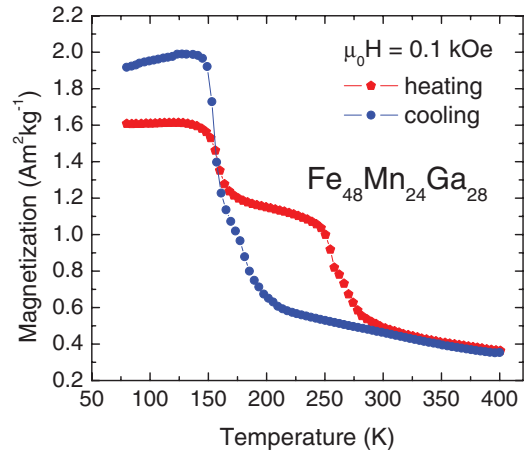


FIG. 2. (Color online) Temperature dependence of the magnetization M measured in a weak (0.1 kOe) magnetic field.

upon cooling and the decrease upon heating apparently reveals that the martensitic transition has a large thermal hysteresis. The large thermal hysteresis between the heating and cooling curves indicates that this transition is of a first order. According to the results of previous studies of $\text{Fe}_{44}\text{Mn}_{28}\text{Ga}_{28}$, $\text{Fe}_{51}\text{Mn}_{22}\text{Ga}_{27}$, and $\text{Fe}_{50}\text{Mn}_{22.5}\text{Ga}_{27.5}$ compositions,^{15,17} this behavior corresponds to a coupled magnetostructural phase transition between ferromagnetic martensite and paramagnetic austenite. In our case of $\text{Fe}_{48}\text{Mn}_{24}\text{Ga}_{28}$, the magnetization M of martensite at 80 K in magnetic field 5 kOe is $M \approx 48 \text{ Am}^2\text{kg}^{-1}$, which is about two times smaller than that for $\text{Fe}_{50}\text{Mn}_{22.5}\text{Ga}_{27.5}$ (Ref. 17). This is not a surprise because the magnetic properties of Fe-Mn-Ga alloys strongly depend on the chemical composition. Due to the presence of a residual martensite, the sample being heated from low temperatures exhibits ferromagnetic behavior even at room temperature. This is clearly seen from both magneto-optical measurements and from the measurements of the magnetic hysteresis loop (inset in Fig. 1). The magneto-optical response at 293 K saturates at $\mu_0 H = 3$ kOe (not shown), which is quite reasonable for martensite inclusions with a small magnetocrystalline anisotropy. It means that in the interval of thermal hysteresis (between 80 and 320 K) and perhaps even in a wider temperature range, martensitic and austenitic phases coexist and their volume fractions gradually change during heating and cooling.

It is interesting to note that the magnetization measured in a weak magnetic field of 0.1 kOe (Fig. 2) demonstrates two marked changes in the slope at heating and only one at cooling. The low-temperature anomaly of M seen on the heating curve at ≈ 150 K can be ascribed to the Curie temperature of the austenitic phase T_C^A . This suggestion is supported by a phase diagram of $\text{Fe}_{72-x}\text{Mn}_x\text{Ga}_{28}$ ($23 \leq x \leq 29$) which showed that in this alloy system, $T_C^A \approx 150$ K is virtually independent of composition.¹⁸ The fact that this anomaly disappears in the stronger magnetic field (Fig. 1) and the absence of any peculiarities on the temperature dependence of the resistivity around 150 K (Fig. 3) indicate that the volume fraction of the residual austenite is rather small at this temperature. Characteristic temperatures of the martensitic transformation, austenite start and finish, A_s and A_f , and martensite start

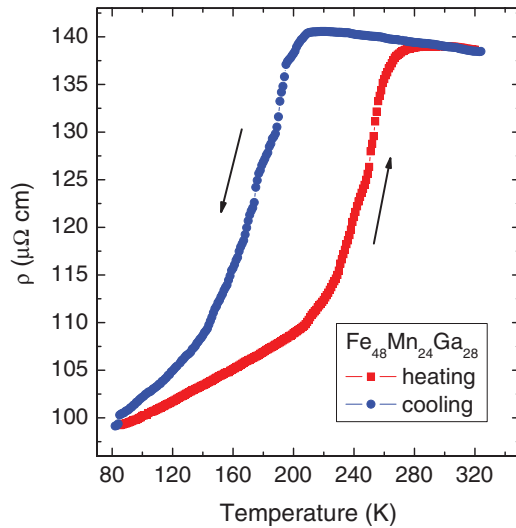


FIG. 3. (Color online) Temperature dependence of the electrical resistivity.

and finish, M_s and M_f , can be estimated from the low-field magnetization data (Fig. 2) as $A_s \sim 143$ K, $A_f \sim 290$ K and $M_s \sim 210$ K, $M_f \sim 141$ K, respectively. It must be noted that this is a rough estimation because the results of magnetic measurements (Fig. 1) indicate that a fraction of the martensite exists even at $T > A_f$.

The results of electrical resistivity measurements (Fig. 3) correlate fairly well with the magnetic measurements (Figs. 1 and 2) and are in good qualitative agreement with the data reported in Ref. 17. Specifically, it is seen from Fig. 3 that at heating, the electrical resistivity ρ increases linearly with temperature up to $T = 210$ K. According to the low-field magnetization data (Fig. 2), this temperature corresponds to the middle of the reverse martensitic transformation. At $T > 210$ K, the volume fraction of the high-temperature paramagnetic austenite exceeds that of the low-temperature ferromagnetic martensite which is accompanied by a rapid growth of ρ . At temperatures above 280 K, the resistivity again demonstrates linear temperature dependence. Upon subsequent cooling from the high temperatures, the linear trend in the resistivity extends down to $T = 205$ K, below which the resistivity rapidly decreases due to the formation of the low-temperature ferromagnetic martensitic phase. The width of thermal hysteresis seen on the $\rho(T)$ dependencies (Fig. 3) accords very well with that revealed by the magnetic measurements (Fig. 1). Temperatures at which the resistivity demonstrates a well-defined change in the slope upon heating and cooling, $T = 280$ K and $T = 205$ K, respectively, are in qualitative agreement with A_f and M_s temperatures determined from the low-field magnetization data (Fig. 2).

It is evident from $\rho(T)$ measured upon cooling (Fig. 3) that electrical resistivity of the austenitic phase, though weak, demonstrates a clear tendency to increase with decreasing temperature, which is not typical for metals. According to the Mooij correlation (for a review, see Ref. 19), $\partial\rho/\partial T < 0$ for high-resistivity metals for which $\rho > \rho^*$, where ρ^* is usually equal to ≈ 150 $\mu\Omega$ cm but can vary from 100 to 300 $\mu\Omega$ cm.

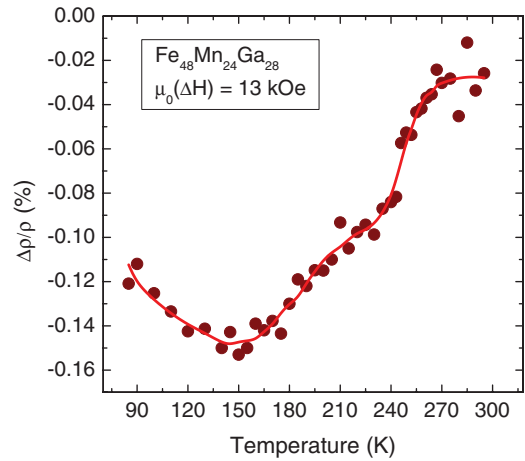


FIG. 4. (Color online) Temperature dependence of the magnetoresistance in a magnetic field $\mu_0(\Delta H) = 13$ kOe.

This correlation has recently been successfully explained by the weak localization in the high-resistivity metals.²⁰ Since the weak localization is suppressed by external or internal magnetic fields, the Mooij correlation is valid only for nonferromagnetic metals. Since ρ in the paramagnetic state of the studied Fe-Mn-Ga alloys is indeed large ($\rho = 140$ $\mu\Omega$ cm in our sample and $\rho = 220$ $\mu\Omega$ cm in the sample studied in Ref. 17), our results are in agreement with this point of view. It is interesting to note that several other Heusler compounds demonstrate negative temperature coefficient of the resistivity, but only in the paramagnetic state.^{7,21} To the best of our knowledge, the only Heusler compounds demonstrating negative temperature coefficient of the resistivity in a weak ferromagnetic state are as-prepared thin films of Co₂MnGe, Co₂MnSi, and Cu₂MnAl with very high (up to 500 $\mu\Omega$ cm) resistivity.⁷ But these thin films in the as-prepared state have very low magnetization (and correspondingly very low internal magnetic fields) and their temperature coefficient of the resistivity becomes positive after annealing when the magnetization increases. This is an additional confirmation that semiconducting behavior of ρ in the high-resistivity metals is due to the weak localization.

The temperature dependence of the magnetoresistance $\Delta\rho/\rho$ measured upon heating protocol for a magnetic field change of 13 kOe is shown in Fig. 4. It is seen that $\Delta\rho/\rho$ is negative in the whole temperature interval of the measurements and ranges from -12% at low temperatures to -0.02% at high temperatures. A local minimum of $\Delta\rho/\rho = -0.15\%$ seen at $T \sim 150$ K correlates well with the additional anomaly of magnetization M measured in the low magnetic field (see Fig. 2). This result clearly indicates that the spin-disorder scattering persists in the whole studied temperature interval.

Examples of Hall resistivity ρ_H of Fe₄₈Mn₂₄Ga₂₈ as a function of the applied magnetic field measured in a temperature interval 80–280 K are shown in Fig. 5. Despite the fact that the reverse martensitic transformation takes place in this temperature range, no abnormal dependence of ρ_H on the magnetic field has been detected. Since the nontrivial behavior of ρ_H reported for Ni-Mn-In (Ref. 11) and

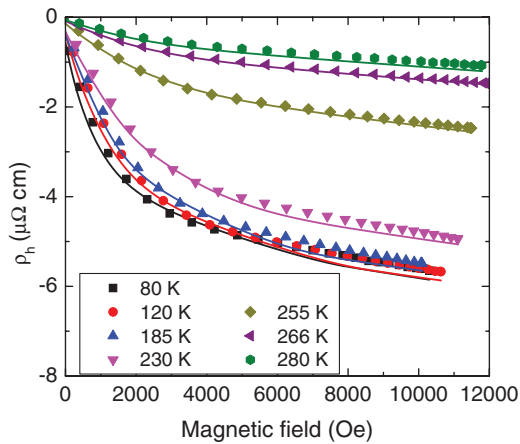


FIG. 5. (Color online) Hall resistivity as a function of the applied magnetic field at different temperatures. Solid lines are a fit to the experimental data.

Ni(Co)-Mn-In (Ref. 12) is due to magnetic-field-induced phase transformation, which is quite common for the ferromagnetic metals shape of the Hall resistivity curves, implies that the magnetic-field-induced phase conversion is virtually absent in the studied $\text{Fe}_{48}\text{Mn}_{24}\text{Ga}_{28}$ alloy. In fact, this is natural to expect, considering that in the alloy studied the magnetic field promotes growth of the ferromagnetic martensite at the expense of paramagnetic austenite.

The distinct feature of the $\text{Fe}_{48}\text{Mn}_{24}\text{Ga}_{28}$ alloy in the low-temperature martensitic phase is a large value of the Hall resistivity ρ_H (Fig. 6). In the magnetic field of 13 kOe, $\rho_H \approx -5.5 \mu\Omega \text{ cm}$ is virtually constant in a temperature interval 80–140 K. At higher temperatures, the absolute value of ρ_H demonstrates a slight decrease up to 240 K where a rapid drop is observed as the temperature is further increased (Fig. 6). The temperature $T = 240$ K at which ρ_H starts to decrease rapidly can also be distinguished at the temperature dependencies of the magnetization M (Fig. 1) and the magnetoresistance $\Delta\rho/\rho$ (Fig. 4). Taking into account the results of magnetic and transport measurements (Figs. 1–4), it can be concluded

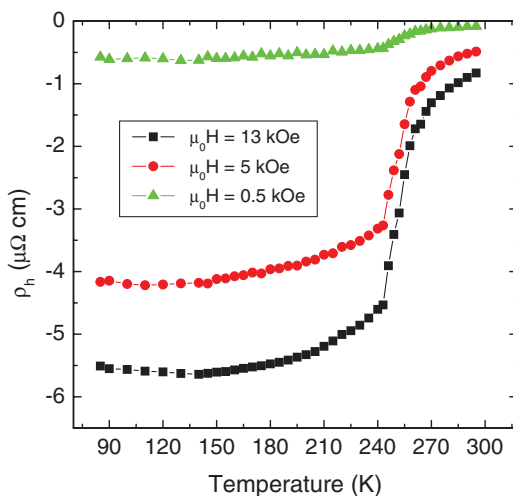


FIG. 6. (Color online) Temperature dependence of the Hall resistivity in different magnetic fields.

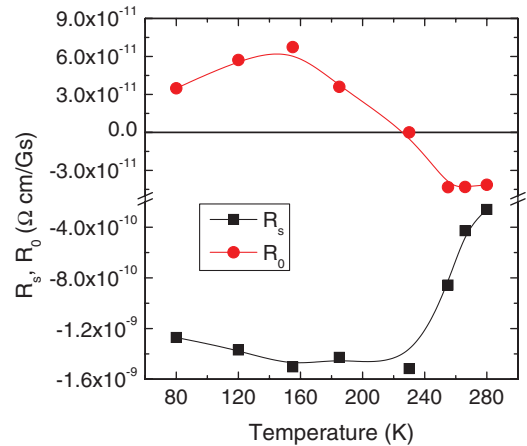


FIG. 7. (Color online) Ordinary R_0 and anomalous R_s Hall coefficients as a function of temperature.

that the rapid decrease of ρ_H at $T > 240$ K is governed by a dominating contribution of the paramagnetic austenite to the Hall resistivity of $\text{Fe}_{48}\text{Mn}_{24}\text{Ga}_{28}$ in the region of the phase coexistence.

The Hall resistivity ρ_H in ferromagnets can be written as a sum of two terms, $\rho_H = R_0 B_z + R_s M_z$, where the first term describes the ordinary Hall effect (OHE), which is related to the Lorentz force, and the second term is the anomalous Hall effect (AHE) resistivity. R_0 and R_s are OHE and AHE coefficients, respectively. Assuming that these coefficients do not depend on magnetization M_z and magnetic induction B_z , which is quite reasonable as a first approximation (at least for low magnetic fields), it is possible to determine these coefficients from experimental ρ_H and M_z data by a fitting procedure. The temperature dependencies of the thus-determined coefficients are shown in Fig. 7.

The temperature dependence of R_s clearly shows that the widely used relations $R_s \sim \rho^2$ (side-jump mechanism or intrinsic contribution; for review, see Ref. 14), $R_s = a\rho + b\rho^2$ (skew scattering¹⁴), or proposed (but not approved by theory) $R_s \sim \rho^{4.0}$ (see Ref. 10 and references therein) for the side-jump mechanism in the case of scattering by large clusters or granules are not valid for the case of $\text{Fe}_{48}\text{Mn}_{24}\text{Ga}_{28}$. For example, as the temperature increases from 240 to 280 K, $|R_s|$ rapidly decreases (Fig. 7), whereas the resistivity ρ increases (Fig. 3). This confirms that there is no universal correlation between R_s and ρ in composites or inhomogeneous ferromagnetic alloys.²² The observed behavior of R_s can be explained qualitatively in the framework of the effective-medium theory^{11,22} as follows. Let us consider our sample as a mixture of austenite and martensite. As follows from Fig. 7, the AHE coefficient for austenite is small. With increasing temperature from 80 to 240 K, the resistivity and the volume fraction of austenite grow simultaneously. These two factors act oppositely on the magnitude of R_s in the $\text{Fe}_{48}\text{Mn}_{24}\text{Ga}_{28}$ sample. Since R_s is a linear function of the austenite fraction but by definition is proportional to ρ^2 , the AHE coefficient R_s increases with temperature. On the contrary, in the temperature range from 240 to 280 K, the amount of austenite increases much more rapidly than the resistivity does and, as a result,

R_s decreases. The general trends in the behavior of R_s and R_0 are similar if one considers the shape of the $|R_s(T)|$ and $R_0(T)$ curves. However, $R_0(T)$ changes more gradually in the temperature interval from 240 to 280 K. It should be noted that since the OHE coefficient is two orders of magnitude smaller than the AEH coefficient, and because R_0 may depend on magnetic field and magnetization,¹³ our results on the behavior of R_0 can be considered as qualitative ones.

IV. CONCLUSION

The study of magnetic, transport, and magnetotransport properties of the Fe₄₈Mn₂₄Ga₂₈ Heusler alloy undergoing coupled magnetostructural phase transition revealed several peculiar features of this material. Specifically, electrical resistivity of the austenitic phase decreases with the increase in temperature, which is uncommon for metals. This feature has been explained as due to the weak localization in the high-resistivity metals.²⁰ The local minimum of the magnetoresistance seen at $T \sim 150$ K originates from the enhanced spin-disorder scattering around the Curie temperature of

the austenitic phase T_C^A which, according to the low-field magnetization measurements (Fig. 2) and the phase diagram of Fe_{72-x}Mn_xGa₂₈ (Ref. 18), is equal to ≈ 150 K.

The value of Hall resistivity ρ_H in Fe₄₈Mn₂₄Ga₂₈ is quite large but several times smaller than in the case suggested for applications Co₂MnAl (Refs. 6 and 9) and nanocomposites²³ with giant Hall resistivity. But there are at least several ways to increase ρ_H significantly, e.g., by increasing magnetization and/or resistivity. For example, it can be done by doping of Fe₄₈Mn₂₄Ga₂₈ with Co and/or by a fabrication of high-resistivity thin films.

ACKNOWLEDGMENTS

This work was partly supported by the Russian Foundation for Basic Research (Grants No. 12-02-00095 and No. 12-02-31297), Russian Ministry of Education and Science (Grant No. 11.519.11.1004), and a Grant-in-Aid for Scientific Research from the Japan Society for the Promotion of Science (JSPS). V.V.K. acknowledges the Creation and Development Program of NUST “MISIS.”

¹T. Graf, S. S. P. Parkin, and C. Felser, *IEEE Trans. Magn.* **47**, 367 (2011).

²A. N. Vasil'ev, V. D. Buchel'nikov, T. Takagi, V. V. Khovailo, and E. I. Estrin, *Phys. Usp.* **46**, 559 (2003).

³P. Entel, V. D. Buchelnikov, V. V. Khovailo, A. T. Zayak, W. A. Adeagbo, M. E. Gruner, H. C. Herper, and E. F. Wassermann, *J. Phys. D: Appl. Phys.* **39**, 865 (2006).

⁴V. A. Chernenko and S. Besseghini, *Sensors Actuators A* **142**, 542 (2008).

⁵*Ferromagnetic Shape Memory Alloys II*, edited by V. A. Chernenko and J. M. Barandiaran (Mater. Sci. Forum, Vol. 635, TTP, Switzerland, 2010).

⁶E. V. Vidal, G. Stryganyuk, H. Schneider, C. Felser, and G. Jakob, *Appl. Phys. Lett.* **99**, 132509 (2011).

⁷M. Obaida, K. Westerholt, and H. Zabel, *Phys. Rev. B* **84**, 184416 (2011).

⁸J. Kubler and C. Felser, *Phys. Rev. B* **85**, 012405 (2012).

⁹Y. J. Chen, D. Basiaga, J. R. O'Brien, and D. Heiman, *Appl. Phys. Lett.* **84**, 4301 (2004).

¹⁰Z. Zhu, S. W. Or, and G. Wu, *Appl. Phys. Lett.* **95**, 032503 (2009).

¹¹I. Dubenko, A. K. Pathak, S. Stadler, N. Ali, Ya. Kovarskii, V. N. Prudnikov, N. S. Perov, and A. B. Granovsky, *Phys. Rev. B* **80**, 092408 (2009).

¹²V. N. Prudnikov, A. P. Kazakov, I. S. Titov, N. S. Perov, A. B. Granovskii, I. S. Dubenko, A. K. Pathak, N. Ali, A. P. Zhukov, and J. Gonzalez, *JETP Lett.* **92**, 666 (2010).

¹³A. Granovsky, V. N. Prudnikov, A. P. Kazakov, A. Zhukov, and I. Dubenko, *J. Exp. Theor. Phys.* **115**, 805 (2012) [*Zh. Exp. Teor. Fiziki* **142**, 916 (2012)].

¹⁴N. Nagaosa, J. Sinova, S. Onoda, A. H. MacDonald, and N. P. Ong, *Rev. Mod. Phys.* **82**, 1539 (2010).

¹⁵T. Omori, K. Watanabe, R. Y. Umetsu, R. Kainuma, and K. Ishida, *Appl. Phys. Lett.* **95**, 082508 (2009).

¹⁶T. Omori, K. Watanabe, X. Xu, R. Y. Umetsu, R. Kainuma, and K. Ishida, *Scripta Mater.* **64**, 669 (2011).

¹⁷W. Zhu, E. K. Liu, L. Feng, X. D. Tang, J. L. Chen, G. H. Wu, H. Y. Liu, F. B. Meng, and H. Z. Luo, *Appl. Phys. Lett.* **95**, 222512 (2009).

¹⁸T. Omori, X. Xu, K. Watanabe, K. Endo, V. V. Khovaylo, K. Ishida, and R. Kainuma (unpublished).

¹⁹J. Gunnarsson, M. Calandra, and J. E. Han, *Rev. Mod. Phys.* **75**, 1085 (2003).

²⁰V. F. Gantmakher, *JETP Lett.* **94**, 626 (2011).

²¹S. Majumdar, M. K. Chattopadhyay, V. K. Sharma, K. J. S. Sokhey, S. B. Roy, and P. Chaddah, *Phys. Rev. B* **72**, 012417 (2005).

²²A. B. Granovsky, A. V. Vedyayev, and F. Brouers, *J. Magn. Magn. Mater.* **136**, 229 (1994).

²³A. B. Pakhomov, X. Yan, and B. Zhao, *Appl. Phys. Lett.* **67**, 3497 (1995).